Biochimica et Biophysica Acta 1798 (2010) 1204–1211

Contents lists available at ScienceDirect

Biochimica et Biophysica Acta

journal homepage: www.elsevier.com/locate/bbamem

Determination of molecular groups involved in the interaction of annexin A5 with lipid membrane models at the air–water interface

Zahia Fezoua-Boubegtiten, Bernard Desbat, Alain Brisson, Sophie Lecomte *

Université de Bordeaux, UMR CNRS 5248 Chemistry and Biology of Membranes and Nano-Objects, Institut Européen de Chimie et Biologie, ENITAB, 2, rue Robert Escarpit F-33607 PESSAC, France

ARTICLE INFO

Article history:
Received 18 November 2009
Received in revised form 4 March 2010
Accepted 17 March 2010
Available online 25 March 2010

Keywords:
Annexin A5
Lipid monolayer
PMIRRAS
BAM
Ellipsometry

ABSTRACT

Annexin A5 (AnxA5) is a member of a family of homologous proteins sharing the ability to bind to negatively charged phospholipid membranes in a Ca^{2+}-dependent manner. In this paper, we used polarization-modulated infrared reflection absorption spectroscopy (PMIRRAS), Brewster angle microscopy (BAM), and ellipsometry to investigate changes both in the structure of AnxA5 and phospholipid head groups associated with membrane binding. We found that the secondary structure of AnxA5 in the AnxA5/Ca^{2+}/lipid ternary complex is conserved, mainly in α-helices and the average orientation of the α-helices of the protein is slightly tilted with respect to the normal to the phospholipid monolayer. Upon interaction between AnxA5 and phospholipids, a shift of the ν_{as} PO_2^- band is observed by PMIRRAS. This reveals that the phosphate group is the main group involved in the binding of AnxA5 to phospholipids via Ca^{2+} ions, even when some carboxylate groups are accessible (PS). PMIRRAS spectra also indicate a change of carboxylate orientation in the aspartate and glutamate residues implicated in the association of the AnxA5, which could be linked to the 2D crystallization of protein under the phospholipid monolayer. Finally, we demonstrated that the interaction of AnxA5 with pure carboxylate groups of an oleic acid monolayer is possible, but the orientation of the protein under the lipid is completely different.

1. Introduction

Annexins comprise a family of eukaryotic proteins that bind to phospholipid membrane in a Ca^{2+}-dependent manner [1]. Several *in vitro* functions including anticoagulatory and anti-inflammatory activities, involvement in signal transduction, in membrane fusion, endo- and exocytosis, and in channel regulation have been described for the annexins, but little is known about their *in vivo* role [2–4]. In addition to regulating the exposure of phosphatidylserine on the outer leaflet of cell membranes, extracellular annexins have been implicated in two basic processes, apoptosis or programmed cell death [5] and platelet activation [6]. The calcium-dependant membrane binding is thought to play a central role in the cellular functions of annexins, and thus, a molecular understanding of this process is an important goal.

Annexin A5 (AnxA5) is the prototype of a family of proteins that share the property of binding to negatively charged phospholipids, in particular phosphatidylserine lipid (PS), in a calcium-dependant manner [7]. It is a 35-kDa soluble protein with an isoelectric point (p*I*) of 4.5. The annexins usually contain 4 or 8 domains with about 70 amino acid residues each. Each domain consists of five α-helices, and the four domains are arranged in a cyclic way, giving the molecule an overall flat, slightly curved shape with the Ca^{2+} binding sites located on the convex membrane-binding face [8–10]. As the function of annexins involves their interactions with biological membranes, the characterization of complexes between annexins and membranes has been performed by many biochemical and biophysical approaches. At the supramolecular level, electron microscopy studies have pointed out the tendency of annexins to self-organize at the surface of biological membranes into 2D-ordered arrays. Annexins A4, A5 [11], and A6 [12] have been shown to spontaneously form 2D crystals on lipid surfaces containing phosphatidylserine. AnxA5 crystallization was performed on lipid monolayers [11] or on supported lipid bilayers [13] of DOPC/DOPS 75%/25% (vol./vol.) mixture. At high calcium concentration (more than 20 mM $CaCl_2$), AnxA5 also crystallized on pure DOPC membranes [14]. Although the formation of AnxA5 2D crystals on supported negatively charged membranes is well characterized, the molecular interaction at the first step of the binding between lipid and protein is not as well described.

The complexity of biological membrane surfaces warrants the use of model membrane systems to investigate interactions between peripheral membranes proteins and phospholipids. Model systems constructed from monolayers rather than vesicles (bilayers) offer greater control over experimental variables such as surface density,

Abbreviations: AnxA5, Annexin A5; BAM, Brewster angle microscopy; PMIRRAS, polarization modulation infrared reflection absorption spectroscopy; DMPS, dimyristoylphosphatidyl-serine

* Corresponding author. Tel.: +33 540003047; fax: +33 540002200.
E-mail address: s.lecomte@cbmn.u-bordeaux.fr (S. Lecomte).

0005-2736/$ – see front matter © 2010 Elsevier B.V. All rights reserved.
doi:10.1016/j.bbamem.2010.03.014

surface pressure, subphase composition, and molecular area. Several techniques were performed to determine the structural and morphological properties of monolayers at the air–water interface, as Brewster angle microscopy [15] (BAM) and infrared reflection–absorption spectroscopy [16] (IRRAS), or polarization-modulated infrared reflection absorption spectroscopy [17] (PMIRRAS). BAM experiments utilize a polarized visible laser to provide optical images of monolayers with a spatial resolution in the μm order. BAM images allow the visualization of the morphology of protein and lipid domains at the air–water interface, as well as changes in lipid monolayer organization after binding of the protein. Ellipsometry measurements allow evaluating the thickness of the layers present at the air–water interface. IRRAS and PMIRRAS give access to the structure of the lipids and the protein secondary structure *in situ* at the air–water interface and offer substantial advantages for studying the interactions of proteins with lipid environments [17,18]. From the PMIRRAS spectra, the orientation of the various secondary structure elements (α-helices or β sheets) can be determined by analyzing the relative intensities of the amide I and amide II bands of the protein monolayers, according to the simulated models [17–20]. Some studies of interactions between AnxA5 and lipid monolayers, using BAM, ellipsometry, or IRRAS spectroscopy were reported in the literature [21–23]. Mukhopadhay and Cho [22] and Andree et al. [23] demonstrated that annexin A5 did not insert into monolayers of various phospholipids. An infrared reflection–absorption spectroscopic study has investigated, at the air–water interface, the secondary structure of AnxA5 as a function of Ca^{2+} and phospholipids in some detail at p*D* 5.6 [24]. Using these conditions, the stabilization of the AnxA5 secondary structure (mainly in α-helices) by DMPA monolayers in the presence of Ca^{2+} was observed. However, no deduction was made regarding the orientation of the protein. During protein adsorption, no change in the lipid conformation was observed in the ternary system [24]. Then, it is now established that the AnxA5 keeps its α-helical structure in a membrane-bound state, but as far as we know, no description of the interactions between phospholipid/Ca^{2+}/AnxA5 at the molecular scale was reported.

The aim of this work was to determine which molecular group of the lipid head group represents the driving force for the interaction with AnxA5 via Ca^{2+}. Although the binding of AnxA5 is stimulated by the presence of PS head group, the protein binding is not specific for this phospholipid [23]. Then, first we managed to study the influence of the electrical charge of the head group of the phospholipids, using the pure zwitterionic DMPC, mixed anionic membrane DMPC/DOPS (80%/20%), and the negatively charged DMPG, comparing with the behavior of AnxA5 under DMPS monolayer. Secondly, we chose to study the interaction of the AnxA5 with the oleic acid monolayer in the presence of Ca^{2+} at pH 7.4 to examine the capacity of binding of AnxA5 to one fatty acid salt monolayer. The current study reports a combined BAM/ellipsometry/PMIRRAS investigation of AnxA5/lipid monolayer/Ca^{2+} interactions. The results clearly demonstrate that the phosphate group is the main group involved in the binding of AnxA5 to phospholipids via Ca^{2+} ions, even when some carboxylate groups are accessible (e.g., PS).

2. Materials and methods

2.1. Chemicals

Dimyristoylphosphatidylserine (DMPS) and dimyristoylphosphatidylcholine (DMPC) were purchased from Avanti Polar Lipids Inc., and dioleoylphosphatidylserine (DOPS), dimyristoyl-phosphatidylglycerol (DMPG), and oleic acid were from Sigma. These lipids were dissolved in a chloroform/methanol mixture (80%/20% vol./vol.) at 0.2 mg/ml. Organic solvents of HPLC grade were purchased from Aldrich (France). Ultrapure water with a nominal resistivity of 18 mΩ·cm (Milli-Q, Millipore) was used for all buffers and solutions. All other chemicals of the highest purity available were purchased from Sigma-Aldrich.

Recombinant AnxA5 was produced according to procedure described by Richter et al. [14] AnxA5 was stored at 4 °C in buffer containing 20 mM Tris–HCl (pH 8), 0.02% NaN_3, and 200 mM NaCl.

2.2. Monolayer formation and surface pressure measurements

Monolayer experiments were performed on a circular Teflon trough (42 cm^2). The surface pressure (π) was measured with a plate of Whatman filter paper held by a Nima Wilhelmy balance. The trough was filled with 8 ml of aqueous buffer containing 10 mM HEPES, 150 mM NaCl, with or without 2 mM $CaCl_2$ (pH 7.4). The temperature was maintained at 26 ± 2 °C for AnxA5 under the lipid monolayers. The interaction of AnxA5 with lipid films was performed in two steps. In the first step, the lipids were spread at the air-water interface from chloroform/methanol (80%/20% vol./vol.) solutions using a Hamilton microsyringe until the surface pressure of 30 mN/m was reached. In the second step, multiple injections of few microliters of the AnxA5 stock solution were performed into the subphase, and the surface pressure was recorded for each protein concentration (29 nM to 200 nM).

2.3. Brewster angle microscopy (BAM) and ellipsometry

BAM images with dimensions 600×450 μm were recorded using a NFT BAM2*plus* Brewster angle microscope (Göttingen, Germany) equipped with a doubled frequency Nd-Yag laser (532 nm, 50 mW), a polarizer, an analyzer, and a CCD camera. The exposure time (ET), depending on the image luminosity, was adjusted to avoid saturation of the camera. The lateral resolution of the BAM pictures with the ×10 magnification lens was about 2 μm, and the BAM images were coded in gray level. To determine the thickness of the layer at the surface, we used the calibration procedure of the BAM software that determines the linear function between the reflectance and the gray level. From the reflectance value, the BAM thickness model allows evaluation of the thickness of the layer at the surface with the knowledge of the experimental Brewster angle and the optical index of the film [25]. For ellipsometric measurements, the same setup as for BAM microscopy was used as an imaging ellipsometer at an incidence angle closed to the Brewster angle (52°). It operates on the principle of classical null ellipsometry [26]. From the angles of the polarizer, compensator, and analyzer, which give the null condition, we can deduce the Δ, Ψ angles that are related to the optical properties of the sample. In ultrathin film conditions, the variation of Δ angle ($\delta\Delta$) is proportional to the film thickness. The comparison of the measured data with computerized optical modeling included in the BAM software leads to a deduction of film thickness when estimation of refractive index can be obtained.

2.4. PMIRRAS spectroscopy

PMIRRAS spectra were recorded on a Nicolet (Madison, WI) Nexus 870 spectrometer equipped with a liquid-nitrogen-cooled mercury cadmium telluride (MCT) detector (SAT, Poitiers) at 77 K with a resolution of 8 cm^{-1}. Six hundred scans representing an accumulation time of 10 min were collected for each spectrum of lipid or AnxA5/lipid monolayers. The optimal value of the angle of incidence for the detection was 75° relative to the optical axis normal to the interface. At this angle of incidence, a negative band indicated a transition dipole moment oriented preferentially perpendicular to the surface, whereas a positive reflection adsorption band was related to a transition dipole moment oriented preferentially in the plane of the surface [17].

We present two types of PMIRRAS spectra depending on the spectrum used for the normalization. PMIRRAS spectra of the sample

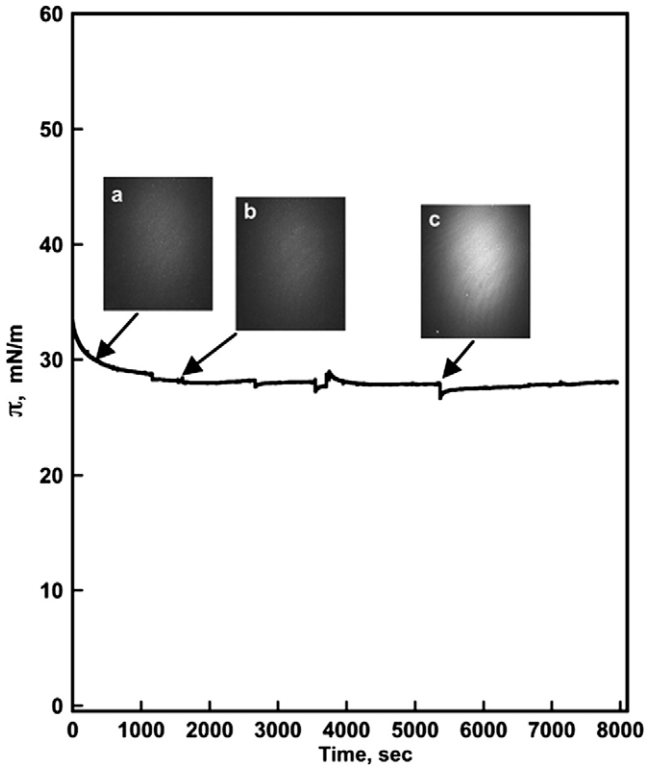

Fig. 1. Variation of lateral surface pressure (π) of a DMPS monolayer (30 mN/m) in function of time at different AnxA5 concentrations. BAM pictures (600×450 μm) of a DMPS monolayer with 2 mM $CaCl_2$: (a) without AnxA5 ($t=5$ min, $\pi=30.6$ mN/m, $R=2.0\times10^{-6}$), (b) with 59 nM AnxA5 ($t=1$ h, $\pi=28.2$ mN/m, $R=2.44\times10^{-6}$), (c) with 148 nM AnxA5 ($t=2$ h, $\pi=27.8$ mN/m, $R=9.89\times10^{-6}$).

normalized by the subphase spectrum or by lipid spectrum are called N_S-PMIRRAS or N_L-PMIRRAS spectra, respectively. N_L-PMIRRAS spectra allow to extract the characteristic contributions of the protein and to detect only the changes in the lipid head groups and acyl chains vibrations induced by the binding of AnxA5 to the lipid monolayers. On such spectra, the nonperturbation of the lipid by the adsorbed protein gives the disappearance of the lipid vibrations. We reported in the Supplementary material the N_S-PMIRRAS spectra of the DMPS in presence of AnxA5 normalized by the subphase spectrum, as usually presented (see Supplementary material Fig. S1 and S2). Thus, the adsorptions of the protein (amide I and amide II bands) superimposed with that of the lipids (carbonyl, CH_2 and the phosphate bands) appear in these spectra.

3. Results

3.1. Interaction of AnxA5 with a DMPS monolayer

A homogeneous condensed film of DMPS monolayer is observed by BAM in the presence or absence of Ca^{2+} (result not shown in absence of Ca^{2+}). A high surface pressure (30 mN/m) reached for the phospholipid monolayers, indicates a high phospholipid packing density. Ellipsometric measurement on the same monolayers gives a variation of the Δ ellipsometric angle (δΔ) of 6° revealing the presence of the lipid monolayer at the interface. Injection of AnxA5 into the subphase, under the DMPS monolayer, in absence of calcium ions did not induce a significant variation of the surface pressure (result not shown). In addition, the small increase of the AnxA5/DMPS film thickness compared to the case of DMPS alone, correlated with a small reflectivity obtained by BAM reveals no binding of the AnxA5 to a DMPS monolayer in the absence of Ca^{2+} (data not shown). This result is rather expected because of the calcium-dependent annexin binding to the membrane.

Fig. 1 shows the temporal variation of lateral surface pressure (π) of DMPS with injection of AnxA5 under the DMPS monolayer in presence of 2 mM Ca^{2+}. No significant variation of surface pressure was observed during time after the different injections of AnxA5. Thus, we conclude that there is no insertion of the protein in the monolayer of DMPS. BAM pictures are also presented in Fig. 1 for different injections of AnxA5 under DMPS monolayer. The AnxA5/Ca^{2+}/DMPS layer remains homogeneous. No domain appears (at the spatial resolution of the Brewster angle microscope), and no segregated domain was formed during the time course of the experiment (2 h) (see Figs. 1b and c). The average reflectance level progressively increased from $R=2.44\times10^{-6}$ to $R=9.89\times10^{-6}$ with addition of AnxA5 from 59 nM to 148 nM, revealing an increase of the layer thickness. Similarly, the variation of the ellipsometric angle ($\delta\Delta=23.7°$) indicates an increase of the layer thickness, comparing with DMPS monolayer alone. The thickness of the film present at the air–water interface can be estimated using the ellipsometric angle or the reflectance value obtained by BAM (see Table 1), for a refractive index value of 1.45. The choice of this refractive index value is explained in the discussion part. The AnxA5/Ca^{2+}/DMPS condensed film thickness was estimated at 55 ± 2 Å and 52 ± 2 Å by ellipsometry and BAM, respectively.

Fig. 2 shows the N_L-PMIRRAS spectra of AnxA5 in interaction with DMPS monolayer at different protein concentrations after stabilization of the phospholipid monolayer, at an initial surface pressure of 30 mN/m, and in presence of 2 mM Ca^{2+}. The amide I band adopts a dispersive like shape with a positive band at around 1653 cm^{-1} indicating that AnxA5 maintains its α-helix structure and an intense positive amide II band was also observed. The dispersive-like shape of

Table 1
Reflectance and (Δ,Ψ) angles values of layers obtained by BAM and Ellipsometry respectively. δΔ, the difference of the angle with (Δ) and without layer ($\Delta_\cdot$) at the air–water interface. The thickness of the film is calculated with a refractive index of 1.45.

Film composition	BAM reflectance ($\times10^{-6}$)[a]	Thickness (Å)	Ellipsometric angle (Δ,Ψ)	$\lvert\delta\Delta\rvert=\lvert\Delta-\Delta_\cdot\rvert$	Thickness (Å)
AnxA5/Ca^{2+}/DMPS	9.89	52	200.90 ± 0.5° 1.79 ± 0.05°	23.70°	55
AnxA5/Ca^{2+}/DMPG	9.83	52	198.90 ± 0.5° 2.05 ± 0.05°	21.70°	50
AnxA5/Ca^{2+}/DMPC-DOPS	11	55	200.50 ± 0.5° 1.90 ± 0.05°	23.30°	55
AnxA5/Ca^{2+}/Oleic acid	9.61	51	200.47 ± 0.5° 1.82 ± 0.05°	23.27°	54
AnxA5/Ca^{2+}/DMPC[b]	ND	ND	348.70 ± 0.5° 2.27 ± 0.05°	13.60°	44

ND: not determined.
[a] Error estimation: 5%.
[b] For the AnxA5/Ca^{2+}/DMPC (Δ,Ψ) ellipsometric angles were determined at an incidence angle of 54.5°. For the other systems, an incidence angle of 52° was used.

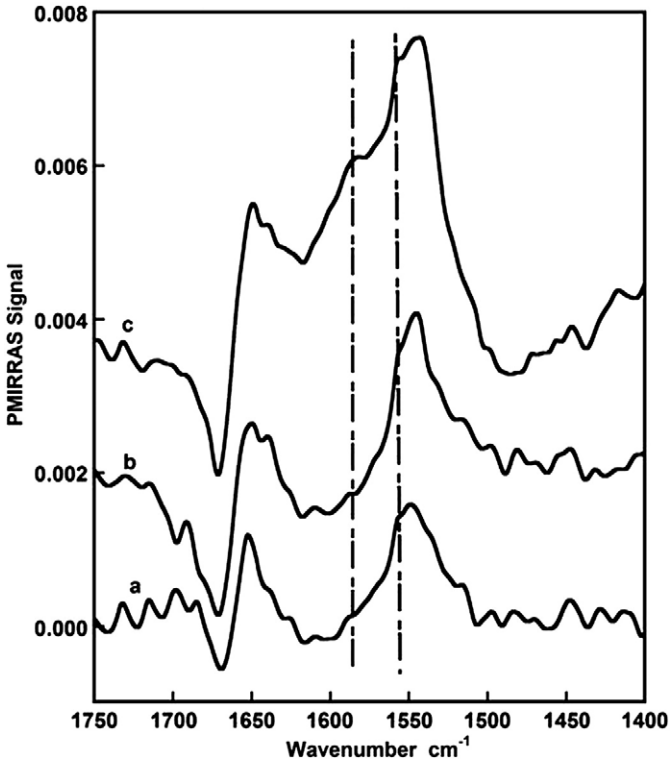

Fig. 2. N_L-PMIRRAS spectra of AnxA5 in interaction with a DMPS monolayer at $\pi = 30$ mN/m in the presence of 2 mM Ca^{2+}: (a) 59 nM AnxA5 ($\pi = 27.4$ mN/m), (b) 89 nM AnxA5 ($\pi = 27.1$ mN/m), (c) 148 nM AnxA5 ($\pi = 27.0$ mN/m). The dashed perpendicular lines showed the bands assigned to the carboxylate antisymmetric vibrations of the aspartate and glutamate residues of the protein. A cutoff of about 2×10^{-3} is made from one spectrum to another.

the amide I band is due to the LO–TO splitting of the amide I mode when the α-helices are out of the plane of the interface. Then, the projection of the α-helices amide I mode along the normal direction gives the LO component of the α-helices at higher wavenumber, and its projection in the plane gives a TO component at lower wavenumber, as described in previous papers [27–30]. We have already observed such spectral shape in the amide I and amide II ranges of AnxA6 [31] studied as function of compression of lipid monolayer. The normalized PMIRRAS spectra of AnxA6 showed a LO–TO splitting of the amide I band and a strong amide II band at higher surface pressure of lipid (27 mN/m), associated with changes in orientation of protein α-helices. Increasing the concentration of AnxA5 leads to higher quantities of protein interacting with the DMPS monolayer via Ca^{2+} ions, as revealed by the increase of the intensity of the PMIRRAS bands. At high protein concentration and at the equilibrium state of the AnxA5 adsorption under DMPS monolayer (Fig. 2c), additional positives absorptions appear at 1555 and 1585 cm^{-1}. Those bands are rather assigned to the carboxylate antisymmetric vibrations of glutamate and aspartate residues of the protein than to the antisymmetric carboxylate band of the head group of DMPS which is situated near 1600 cm^{-1} and is very broad (see Fig. S2b). Moreover, at the end of the AnxA5 adsorption process, the antisymmetric vibrations of the carboxylates residues are correlated with the presence of one band at around 1410 cm^{-1} of low intensity assigned to the carboxylate symmetric vibrations (observable also in the 1450–950 cm^{-1} range; Fig. 3c). Using the previously calculated normalized PMIRRAS spectra [17–20] in the amide I and amide II regions for pure α-helices, we have plotted the variation of the amide I/amide II ratio (AI/AII) as function of the tilt angle, θ, between the helices axis and the normal to the interface (curve r_a), as usually presented (see Supplementary material Fig. S3). The AI/AII ratio was calculated using the intensities at the maxima of the positive components of amide I and amide II bands. The AI/AII ratio was used to estimate the relative orientation changes of protein molecules. The average orientation of the α-helices axis of AnxA5 molecules adsorbed under the DMPS was evaluated assuming that most of amide groups in the monolayer have a helical secondary structure. From the curve r_a (Fig. S3), the AI/AII ratio of 0.7 measured for the AnxA5 under DMPS and the formation of a negative band at 1670 cm^{-1} (Fig. 2c) indicate an average orientation of 30° of the α-helices axis with respect to the normal to the interface (60° with respect to the interface plane). This result is in agreement with the orientation obtained for a bacteriorhodopsin monolayer [32] with a similar shape of PMIRRAS spectrum. The bacteriorhodopsin monolayer spread at the air-water interface possesses α-helices with an average tilt angle of 26° with respect to the normal to the interface (64° with respect to the interface plane) [32]. To better confirm the helix orientation, we have tried to reproduce the experimental spectrum of AnxA5 interacting with DMPS monolayer by adjusting our optical anisotropic indices of α-helices reported previously [20,33]. Then, various simulations were performed assuming that the crystalline structure of AnxA5 presents essentially two populations of helices, perpendicular and parallel to the average plane of the protein. The theoretical spectrum, which best fits the experimental amide I band profile of AnxA5 under DMPS (Fig. S4), corresponds to a specific orientation of protein α-helices under lipid monolayer with 70% of the α-helices oriented perpendicularly to the interface and 30% oriented in the plane of the phospholipid monolayer. This structural distribution is in good agreement with the orientation of the alpha helices in the crystalline structure of AnxA5. Finally, we report (Fig. 3) the N_S and N_L-PMIRRAS spectra in the range 1450–950 cm^{-1} where the symmetric and antisymmetric PO_2^- vibrations of the lipid are observed. The hydrated antisymmetric PO_2^- vibrations of the DMPS monolayer (Fig. 3a) without calcium gives an intense band observed at 1219 cm^{-1}. Addition of 2 mM Ca^{2+} induces a small shift of this band to 1225 cm^{-1} (Fig. 3b).

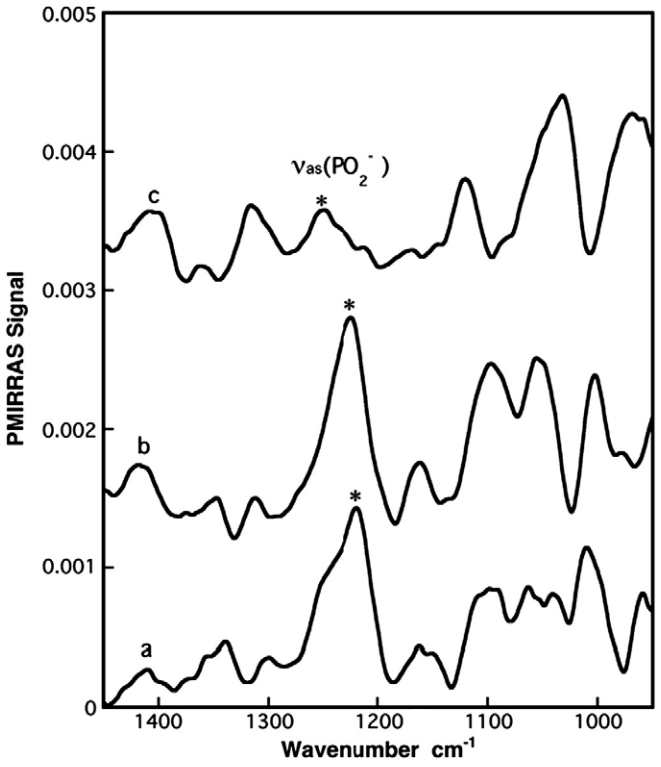

Fig. 3. N_S-PMIRRAS spectra of a DMPS monolayer ($\pi = 30$ mN/m): (a) in absence of calcium, (b) with 2 mM $CaCl_2$, (c) N_L-PMIRRAS spectrum of AnxA5 (148 nM) in interaction with a DMPS monolayer ($\pi = 27$ mN/m) in the presence of 2 mM Ca^{2+}.

The changes in the lipid head groups induced by the binding of AnxA5 to the lipid monolayers are revealed on N_L-PMIRRAS (Fig. 3c). The weak band observed at 1250 cm^{-1} reveals the perturbation of PO_2^- groups due to the binding of AnxA5. Even if it is difficult to understand all the modifications in the spectral range of the PO_2^- symmetric stretching, the large band observed at around 1040 cm^{-1} indicates also a modification of the orientation of the POC ester group during AnxA5 adsorption. Moreover, the binding of AnxA5 to the DMPS/Ca^{2+} complex gives rise to the appearance of one band at 1121 cm^{-1}, which is probably due to a change of the vibrational couplings between POP, POC, and CC stretching bonds during the conformational modification of the ester phosphate head group [34].

3.2. Interaction of AnxA5 with monolayers of different phospholipids

Monolayers of various charged head group phospholipids (DMPC, DMPG, DMPC/DOPS mixture) have been investigated to compare with the specificity of the DMPS to the AnxA5 binding. All the figures (BAM images and PMIRRAS spectra) of this part are shown in the Supplementary material. At first, without Ca^{2+}, no adsorption of AnxA5 was observed whatever the lipid monolayer used (data not shown). Secondly, AnxA5 does not bind to DMPC monolayer with only 2 mM Ca^{2+}, as already observed [14,35,36]. Calcium concentration was then increased to about 100 mM with DMPC monolayer [36]. Then, for each system in the presence of Ca^{2+}, a homogeneous condensed film was observed by BAM at the air–water interface (Fig. S5). The film thicknesses (lipid/Ca^{2+}/AnxA5) were calculated (see Table 1). Similar values (50 Å or 55 Å) are obtained except for the DMPC/Ca^{2+}/AnxA5 layer (44 Å). Thus, a lower binding of AnxA5 on pure PC lipid can be suggested, in agreement with the smaller amide bands intensities obtained on PMIRRAS spectra (see below). The injections of AnxA5 under DMPC/DOPS (80%/20%) or DMPC monolayers induce no variation of lateral surface pressure (π) (result not shown), as in the case of DMPS. With DMPG monolayer, an increase of surface pressure from 30 to 38 mN/m is observed after binding of AnxA5.

The N_L-PMIRRAS spectra of AnxA5 in interaction with DMPC or DMPC/DOPS monolayers (Figs. S6a and b) in the presence of calcium show a similar shape of the amide I and amide II bands as with DMPS. The amide I peak is centered at 1651 cm^{-1} which is characteristic of the α-helix structure of AnxA5, and the amide I/amide II ratio is rather low (0.5 at 0.7) close to the value obtained in the case of AnxA5 under DMPS (0.7). The N_L-PMIRRAS spectrum of AnxA5 under a DMPG monolayer (Fig. S6c) shows a broad negative component around 1630 cm^{-1} in addition to the amide I and amide II bands. This spectral deformation reveals, presumably, the perturbation of water molecular layer between the DMPG and the protein. However, the ratio of the amide I/amide II bands is still low. As with DMPS, some modifications are observed in the N_L-PMIRRAS spectra of AnxA5 under DMPC, DMPG or DMPC/DOPS monolayers in the spectral range of the phosphate vibrations (see Fig. S7). Indeed, the binding of AnxA5 to DMPC or DMPG monolayers induces a larger shift of 10 cm^{-1} to higher wavenumbers of the antisymmetric PO_2^- stretching mode, compared with its binding to DMPS. Slight differences can be observed for DMPG, which presents only one negative charge. A reorientation of the phosphate group in the plane of the interface is observed on PMIRRAS spectra. In addition, an important increase of the intensity of the symmetric PO_2^- stretching (1085 cm^{-1}) and POC stretching (1045 cm^{-1}) modes are observed. The change of the phosphate orientation probably results from a favored access of Ca^{2+} to the phosphate group in the phosphatidylglycerol head group of DMPG compared with serine head group of DMPS. The increase of lateral surface pressure ($\Delta\pi = 8$ mN/m) of the DMPG monolayer may be related to a reorientation of the lipid phosphate group in the plane of the interface due to its binding with AnxA5. The N_L-PMIRRAS spectrum of the AnxA5 interacting with a mixed DMPC/DOPS (80%/20%) lipid (Fig. S7b) shows a weak absorption in the phosphate frequencies domain probably due to the low proportion (20%) of PS phospholipid, which can interact with the protein at this calcium concentration (2 mM Ca^{2+}).

3.3. Interaction of AnxA5 with monolayer of oleic acid

We chose to study the interaction of the AnxA5 with the oleic acid salt monolayer in the presence of Ca^{2+} to examine the binding capacity of AnxA5 to carboxylate group, which is the only negatively charged binding site in this case. Fig. 4 shows BAM pictures of an oleic acid monolayer at the air–water interface (Fig. 4a) and after injection of AnxA5 (Figs. 4b and c). Different domains are formed in presence of a low concentration of AnxA5 (Fig. 4b). At a higher concentration of AnxA5 (110 nM), the film at the interface is more condensed and seems more homogeneous (Fig. 4c). The reflectivity increases

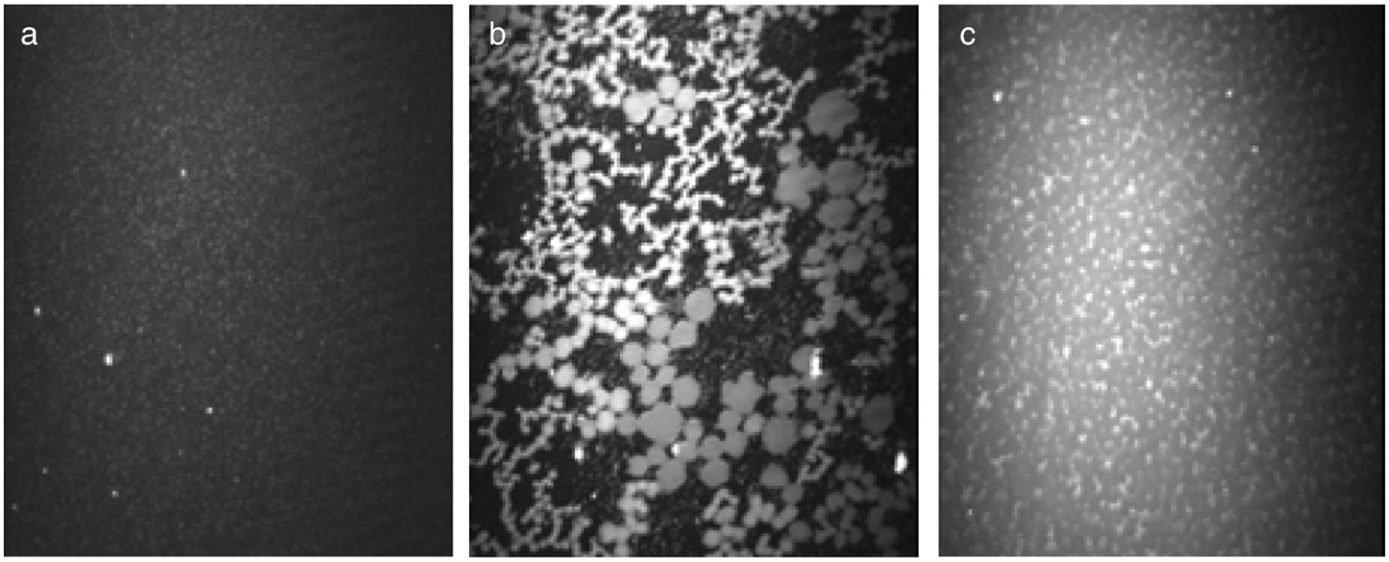

Fig. 4. BAM pictures of an oleic acid monolayer at the air–water interface in the presence of 2 mM $CaCl_2$: (a) without AnxA5 ($t = 6$ min, $\pi = 19.3$ mN/m, $R = 1{,}14 \times 10^{-6}$), (b) with 55 nM AnxA5 ($t = 44$ min, $\pi = 19$ mN/m, $R = 3.48 \times 10^{-6}$), (c) with 110 nM AnxA5 ($t = 2$ h 13 min, $\pi = 19$ mN/m, $R = 9.61 \times 10^{-6}$).

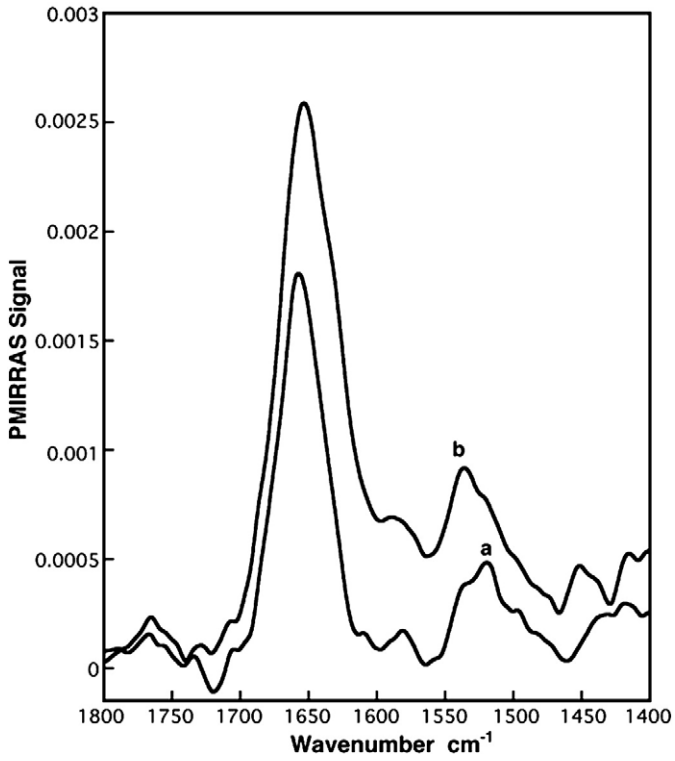

Fig. 5. N_L-PMIRRAS spectra of AnxA5 in interaction with an oleic acid monolayer ($\pi = 30$ mN/m) recorded in the presence of 2 mM $CaCl_2$: (a) $t = 1$ h, $\pi = 30$ mN/m, (b) $t = 2$ h, $\pi = 30$ mN/m.

and reaches a value of 9.61×10^{-6}. The thickness of the film was estimated at 54 ± 2 Å by ellipsometry, which is comparable to the BAM estimation (51 Å; see Table 1).

To go further in the organization of AnxA5 under the oleic acid monolayer, N_L-PMIRRAS spectra of AnxA5 adsorbed under the oleic acid film in presence of 2 mM Ca^{2+} were collected at different concentrations of AnxA5 (Fig. 5). The sharp amide I band at 1650 cm^{-1} indicates the conservation of the α-helices structures of the AnxA5 under the oleic acid monolayer but the shapes of the amide I and amide II bands are different compared to the amide profiles, described above for AnxA5 under phospholipid monolayers. Positive amide I and amide II bands are observed with a ratio AI/AII equal to 3, which is completely different of the 0.7 value observed in presence of phospholipids. From the curve r_a (Fig. S3), we can deduce that the α-helices axis of the AnxA5 is mainly tilted with an average angle of 60° with respect to the normal to the interface (30° with respect to the interface plane). This result should be regarded as indicative, given the assumption mentioned above concerning the helical secondary structure. On another hand, in spite of the same thickness evaluated under DMPS monolayer, the orientation of AnxA5 under the oleic acid monolayer is completely different.

4. Discussion

In this current study, the pictures provided by BAM supplemented with the molecular structural data provided by surface pressure and PMIRRAS measurements offer a unique set of tools for monitoring the spatial and temporal organization of both the proteins and lipids in monolayer film at the air–water interface. Ca^{2+} at 2 mM promotes AnxA5 binding to phospholipid monolayers except for pure PC monolayers, as already reported by other authors [14,23]. The high reflectivity obtained and the increase of the film thickness reveals the formation of a layer of AnxA5 under the used phospholipids. The calcium-dependent interaction of AnxA5 with membrane bilayers and monolayers is widely considered to be peripheral [37]. In support of this peripheral mechanism, our spectroscopic measurements, including surface pressure and ellipsometry, rule out significant insertion of the AnxA5 into the lipid monolayer. Our results are consistent with the idea that binding of AnxA5 to phospholipid monolayers mediated by Ca^{2+} is largely driven by specific interactions without substantial membrane penetration, as suggested by other authors [22,38]. However, Wu et al. [21] observed a dynamic change of DMPA lipid films due to the AnxA5 binding. The differences could be explained by the nature of anionic phospholipids and also by the difference of the physical state of the phospholipid films. Phospholipids were in the LE/LC phase transition region in the Wu et al. [21] study, whereas the phospholipid films employed in our study were in liquid condensed phase. With the observed reflectance and ellipsometric measurements, we estimated the thickness of the film formed at the interface. The determination of the film thickness mainly depends on the refractive index used [39]. Since it is difficult to determine an accurate experimental refractive index value, we therefore decided to use the same average value of the refractive index for both lipid layers and AnxA5 to reduce the number of parameters introduced in our model. The lacunal structure of the two-dimensional crystals of annexin A5 formed on phospholipid bilayers and monolayers including a large aqueous space [38,40–43] leads us to choose a low refractive index of 1.45 to take into account the large presence of water. Then, we estimated the thickness of all the lipid monolayers used in this work at 20 Å. The same thickness, around 55 Å, was obtained for films of AnxA5/Ca^{2+}/DMPS, AnxA5/Ca^{2+}/DMPC–DOPS, or AnxA5/Ca^{2+}/DMPG. Then, the thickness of the AnxA5 under these monolayers was calculated at 35 Å. According to the crystalline AnxA5 structure in the presence of Ca^{2+} [9,10], this thickness corresponds to the height of AnxA5.

PMIRRAS was useful to determine the structure and the orientation of the AnxA5 under these different lipid monolayers. Ca^{2+} favors strongly the auto-organization of the protein and stabilizes its highly α-helical structure (sharp amide-I band, centered at 1651 cm^{-1}). The AnxA5 adopts a specific orientation under lipid monolayers, with some 70% of α-helices oriented perpendicularly to the interface and 30% in the plane of the phospholipid monolayer, for each studied monolayer. This structural distribution is in good agreement with the projection of the α-helices of crystallized AnxA5 in presence of Ca^{2+} [9,10] on the principal axes of the protein. Fig. 6 presents a scheme of the orientation of AnxA5 under the phospholipid monolayer via Ca^{2+} in the (z,y) plane (scheme a), in the (x,y) plane (scheme b). Thus, the estimated thickness value of AnxA5 (35 Å) in the ternary system is also in agreement with this orientation of the AnxA5 under phospholipid monolayer in the (z,y) or (x,y) plane. High-resolution images from cryoelectron microscopy already showed that the overall structure of AnxA5 remains similar to the X-ray crystal structure upon binding to the membrane [38,40]. Circular dichroism spectra of AnxA5 in the presence or absence of phospholipid vesicles containing mixture of phosphatidic acid (PA) and phosphatidylcholine (PC) and in the presence of calcium have shown no significant conformational change of AnxA5 upon its binding to the vesicles [44]. The authors also revealed that the protein induced a change in the vesicle morphology that corresponds to reduced membrane curvature [44]. The present study shows no change in the order of the lipid acyl chains in the ternary complex probably due to the initial rigid structure of DMPS monolayer at high surface pressure, in its LC phase (see results and Fig. S1 in the Supplementary material). Likewise, no protein effect on the lipid carbonyl groups was observed during the adsorption of AnxA5 to DMPS-Ca^{2+} monolayers (see results and Fig. S2 in the Supplementary material).

All the phospholipids used have a phosphate group in common. PMIRRAS spectra reveal that both Ca^{2+} and AnxA5 mainly affect this phosphate group. Casal et al. [45] established a correlation between the state of hydration of the phosphate group and its mobility in

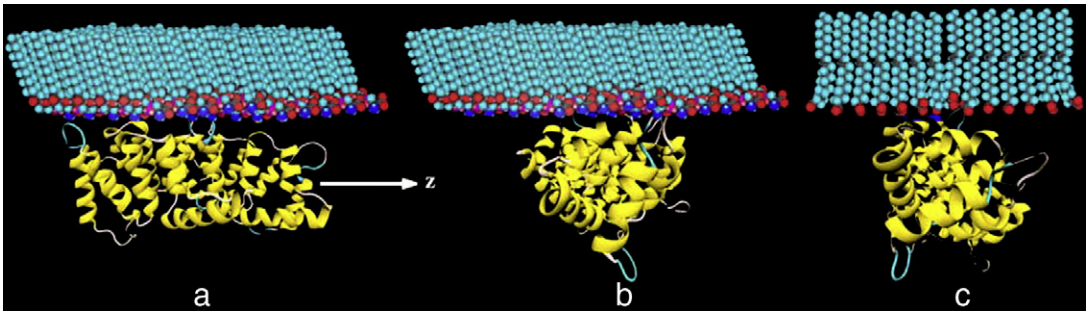

Fig. 6. Schemes of orientation of AnxA5 in the presence of Ca^{2+}: (a) under phospholipid, projection in the (*z*,*y*) plane; (b) under phospholipid, projection in the (*x*,*y*) plane; (c) under oleic acid, projection in the (*x*,*y*) plane.

presence of Ca^{2+}, by infrared and ^{31}P NMR. Ca^{2+} binds to the phosphate group, replacing the water of hydration of the phosphate group and leading to its immobilization [45,46]. We demonstrate here that binding of AnxA5 to lipid via Ca^{2+} increases the phenomenon of dehydration of the phosphate group, as revealed by the shift of the bands from 1225 cm^{-1} to 1250 cm^{-1} for DMPS and to 1260 cm^{-1} for DMPC, DMPG, respectively.

The observation of the negative charged aspartate and glutamate residues of the AnxA5 interacting with DMPS points out the specific organization of the protein. Most of the time, the corresponding vibrations were not observed in the PMIRRAS spectra of proteins but two parameters may favor their observation. First, AnxA5 contains a large proportion of aspartates (27 of 319 residues in protein) and glutamates (28 of 319 residues in protein) residues. Secondly, the self-assembled AnxA5 under DMPS monolayer, forming a condensed film, should organize and orient the carboxylate groups of these amino acids residues. PMIRRAS is sensitive to the orientation of transition dipole moments and favors the observation of vibrations, which have their transition dipole moments in the plane of the interface [17]. In consequence, the observation of both $\nu_{as}COO^-$ (between 1555 and 1585 cm^{-1}) and $\nu_s COO^-$ (around 1410 cm^{-1}) suggests that the carboxylate transition dipole moments are mainly oriented in the plane of the interface at the final step of AnxA5 adsorption.

All the results presented in this paper allow us to conclude that AnxA5 interacts predominantly with the phosphate group of the lipid rather than with the other negative groups such as the carboxylate of the serine polar head group. Swairjo and Seaton [47] demonstrated that the distance between phosphate and Ca^{2+} is smaller than between COO^- and Ca^{2+} in the crystal complex of AnxA5/Ca^{2+}/GPS or GPE (glycerophosphatidylserine or glycerophosphoethanolamine). The results obtained for the binding of AnxA5 to an oleic acid monolayer emphasize this conclusion. On a negative group such as carboxylate, AnxA5 is able to form a monolayer of proteins with similar thickness (34 Å) compared under phospholipids. However, we demonstrate by PMIRRAS that the orientation of the AnxA5 is completely different. The α-helices are maintained, but they are oriented mainly tilted with an angle of 60° with respect to the normal to the interface, which also differs from the orientation of crystallized AnxA5 on membranes. These results suggest a rotation of the AnxA5 along its long-axis *z*. Indeed, the shape of the AnxA5 is almost cylindrical. So, the change from its organization under phospholipids (α-helices mainly vertical; Fig. 6b) to its structure under oleic acid (α-helices mainly at 30° of the interface plane; Fig. 6c) can simply be done by a reorientation along the *z* direction. With this organization, the protein keeps almost the same thickness (34 Å), in agreement with the ellipsometric data, and the α-helices are mainly in the interface plane, in agreement with the PMIRRAS spectra. This orientation is different from the well-known crystalline structure of the protein under phospholipids.

In summary, the results of this study clearly establish that the main driving force for the AnxA5 interaction with lipid is the fixation of Ca^{2+} on the phosphate group of the phospholipid as DMPS, DMPC, or DMPG. Even if we demonstrated the possibility of interaction between carboxylate and AnxA5, the carboxylate group of the phospholipids polar heads (DMPS, DOPS) plays a minimal role in the interaction of the protein with these phospholipids via calcium ions, in spite of its closer proximity with the solvent. We propose the following molecular model of a Ca^{2+}-dependent association of AnxA5 with membranes. In the first step, Ca^{2+} induces removal of the hydration water of the phospholipid phosphate groups leading to the immobilization of the phosphate groups. We demonstrate that there is no insertion of the AnxA5 in the lipid monolayer and that the α-helices of the AnxA5 are uniformly oriented under the phospholipid monolayer, as 70% and 30% oriented perpendicular and parallel to the monolayer, respectively (see Fig. 6a). Secondly, the carboxylate groups of the aspartate and glutamate residues of the protein are involved in the final self-association of the AnxA5 under the lipid monolayer, as experimentally revealed by PMIRRAS. Presently, we cannot establish if the self-association of AnxA5 is due only to the interaction between carboxylate of glutamate or aspartate via bridging of Ca^{2+} or if the carboxylate of the amino acids interact with other amino acids charged positively as lysine or arginine. Finally, our data obtained with the oleic acid monolayer show the possibility to stabilize the AnxA5 at the air–water interface in a new orientation.

Acknowledgments

The authors wish to thank Céline Gounou, assistant engineer (IECB, Alain Brisson team, Bordeaux, France) for providing recombinant AnxA5.

Appendix A. Supplementary data

Supplementary data associated with this article can be found, in the online version, at doi:10.1016/j.bbamem.2010.03.014.

References

[1] E. Moss, The Annexins Ed, Portland Press, London, 1992.
[2] V. Gerke, C.E. Creutz, S.E. Moss, Annexins: linking Ca^{2+} signalling to membrane dynamics, Nat. Rev. Mol. Cell Biol. 6 (2005) 449–461.
[3] P. Raynal, H.B. Pollard, Annexins: the problem assessing the biological role for a gene family of multifunctional calcium-and phospholipid-binding proteins, Biochim. Biophys. Acta 1197 (1994) 63–93.
[4] V. Gerke, S.E. Moss, Annexins: from structure to function, Physiol. Rev. 82 (2002) 331–371.
[5] V. Fadok, D.R. Voelker, P.A. Campbell, J.J. Cohen, D.L. Bratton, P.M. Henson, Exposure of phosphatidylserine on the surface of apoptotic lymphocytes triggers specific recognition and removal by macrophages, J. Immunol. 148 (1992) 2207–2216.
[6] E.M. Bevers, P. Comfurius, R.F.A. Zwaal, Changes in membrane phospholipid distribution during platelet activation, Biochim. Biophys. Acta 736 (1983) 57–66.
[7] P. Meers, Annexin binding to lipid assemblies, in: B.A. Seaton (Ed.), Annexins: Molecular Structure to Cellular Function, R. G. Landes. Company, Austin, TX, 1996, pp. 97–119.

[8] R. Huber, J.M. Römisch, E.P. Paques, The crystal and molecular structure of human annexin V, an anticoagulant protein that binds to calcium and membranes, EMBO J. 9 (1990) 3867–3874.
[9] N.O. Concha, J.F. Head, M.A. Kaetzel, J.R. Dedman, B.A. Seaton, Rat annexin V crystal structure: Ca^{2+}- induced conformational changes, Science 261 (1993) 1321–1324.
[10] J. Sopkova, M. Renouard, A. Lewit-Bently, The crystal structure of a new high-calcium form of annexin V, J. Mol. Biol. 234 (1993) 816–825.
[11] F. Oling, W. Bergsma-Schutter, A. Brisson, Trimers, dimers of trimers, and trimers of trimers are common building blocks on annexin A5 two-dimensional crystals, J. Struct. Biol. 133 (2001) 55–63.
[12] H.P.C. Driessen, R.H. Newman, P.S. Freemont, M.J. Crumpton, A model of the structure of human annexin VI bound to lipid monolayers, FEBS Lett. 306 (1992) 75–79.
[13] I. Reviakine, W. Bergsma-Schutter, A. Brisson, Growth of protein 2-D crystals on supported planar lipid bilayers imaged *in situ* by AFM, J. Struct. Biol. 121 (1998) 356–361.
[14] R.P. Richter, J. Lai Kee Him, B. Tessier, C. Tessier, A.R. Brisson, On the kinetics of adsorption and two-dimensional self-assembly of annexin A5 on supported lipid bilayers, Biophys. J. 89 (2005) 3372–3385.
[15] D. Vollhardt, Morphology and phase behaviour of monolayers, Adv. Colloid Interface Sci. 64 (1996) 143–171.
[16] R.J.W. Mendelsohn, J.W. Brauner, A. Gericke, External infrared reflection absorption spectroscopy monolayer films at the air water interface, Annu. Rev. Phys. Chem. 41 (1995) 441–476.
[17] D. Blaudez, J.M. Turlet, J. Dufourcq, D. Bard, T. Buffeteau, B. Desbat, Investigations at the air/water interface using polarization modulation IR spectroscopy, J. Chem. Soc.-Faraday 92 (1996) 525–530.
[18] I. Cornut, B. Desbat, J.M. Turlet, J. Dufourcq, *In situ* study by polarization modulated Fourier transform infrared spectroscopy of the structure and orientation of lipids and amphipathic peptides at the air-water interface, Biophys. J. 70 (1996) 305–312.
[19] H. Lavoie, J. Gallant, M. Grandbois, D. Blaudez, B. Desbat, F. Boucher, C. Saless, The behavior of membrane proteins in monolayers at the gas–water interface: comparison between photosystem II, rhodopsin and bacteriorhodopsin, Mat. Sci. Eng. C Bio. 10 (1999) 147–154.
[20] T. Buffeteau, D. Blaudez, E. Péré, B. Desbat, Optical constant determination in the infrared of uniaxially oriented monolayers from transmittance and reflectance measurements, J. Phys. Chem. B 103 (1999) 5020–5027.
[21] F. Wu, G. Arne, C.R. Flach, T.R. Mealy, B.A. Seaton, R. Mendelsohn, Domain structure and molecular conformation in annexin V/ 1, 2- dimyristoyl-*sn*-glycero-3-phosphate/Ca^{2+} aqueous monolayers: a Brewster angle microscopy/infrared reflection–absorption spectroscopy study, Biophys. J. 74 (1998) 3273–3281.
[22] S. Mukhopadhay, W. Cho, Interaction of annexin V with phospholipid monolayers, Biochim. Biophys. Acta 1279 (1996) 58–62.
[23] H.A.M. Andree, C.P.M. Reutelingsperger, R. Hauptman, H.C. Hemker, W.T. Hermens, G.M. Willems, Binding of vascular anticoagulant alpha (VAC alpha) to planar phospholipid bilayers, J. Biol. Chem. 265 (1990) 4923–4928.
[24] F. Wu, C.R. Flach, B.A. Seaton, T.R. Mealy, R. Mandelsohn, Stability of annexin V in ternary complexes with Ca^{2+} and anionic phospholipids: IR studies of monolayer and bulk phases, Biochemistry 38 (1999) 792–799.
[25] M.N.G. De Mul, J.A. Mann, Determination of the thickness and optical properties film from the domain morphology by Brewster angle microscopy, Langmuir 14 (1998) 2455–2466.
[26] R.M.A. Azzam, N.M. Bashara, Ellipsometry and polarized light, North-Holland Physics publishing, New York, 1977.
[27] M. Balkansky, in: Abeles (Ed.), Optical properties of solids, North Holland Publishing Company, 1972, Chap 8.
[28] P.T. Griffiths, J.A. de Haseth, Fourier transform infrared spectrometry, Wiley, New York, 1986, p. 295.
[29] K. Yamamoto, H. Ishida, Optical theory applied to infrared spectroscopy, Vibrational Spectrosc. 8 (1994) 1–36.
[30] T. Hasegawa, J. Nishijo, J. Umemura, W. Theiss, Simultaneous evaluation of dielectric dispersion and molecular orientation in thin condensed matters by infrared spectroscopy, Anal. Sci. 17 (2001) 697–700.
[31] M. Golczac, A. Kirilenko, J. Bandorowicz-Pikula, B. Desbat, S. Pikula, Structure of human annexin A6 at the air–water interface and in a membrane-bound state, Biophys. J. 87 (2004) 1215–1226.
[32] D. Blaudez, F. Boucher, T. Buffeteau, B. Desbat, M. Grandbois, C. Salesse, Anisotropic optical constants of bacteriorhodopsin in the mid-infrared: consequence on the determination of α-helix orientation, Appl. Spectrosc. 53 (1999) 1299–1304.
[33] T. Buffeteau, E. Le Calvez, S. Castano, B. Desbat, D. Blaudez, J. Dufourcq, Anisotropic optical constants of α-helix and β-sheet secondary structures in the infrared, J. Phys. Chem. B 104 (2000) 4537–4544.
[34] H. Binder, K. Köhler, K. Arnold, O. Zschörnig, pH and Ca^{2+} dependent interaction of Annexin V with phospholipid membranes: a combined study using fluorescence techniques, microelectrophoresis and infrared spectroscopy, Phys. Chem. Chem. Phys. 2 (2000) 4615–4623.
[35] P. Meers, T. Mealy, Relationship between annexin V tryptophan exposure, calcium and phospholipid binding, Biochemistry 32 (1993) 5411–5418.
[36] N. Govorukhina, A. Bergsma-Schutter, C. Mazères-Dubut, S. Mazères, E. Drakopoulou, L. Bystrykh, F. Oling, A. Mukhopadhyay, I. Reviakine, J. Lai Kee Him, A. Brisson, Self-assembly of annexin A5 on lipid membranes, in: J. Bandorowicz-Pikula (Ed.), Annexins: Biological importance and annexin-relatedpathologies, Landes Bioscience/ Eurekah. com, Georgetown, TX, 2003, pp. 37–55.
[37] M.A. Swairjo, B.A. Seaton, Annexin structure and membrane interactions: a molecular perspective, Annu. Rev. Biophys. Biomol. Struct. 23 (1994) 193–213.
[38] D. Voges, R. Berendes, A. Burger, P. Demange, W. Baumeister, R. Huber, Three-dimensional structure of membrane-bound annexin V—a correlative electron microscopy–X-ray crystallography study, J. Mol. Biol. 238 (1994) 199–213.
[39] D. Ducharme, J.J. Max, C. Salesse, R.M. Leblanc, Ellipsometric study of the physical state of phosphatidylcholines at the air–water interface, J. Phys. Chem. 94 (1999) 1925–1932.
[40] A. Brisson, G. Mosser, R. Huber, Structure of soluble and membrane-bound human annexin V, J. Mol. Biol. 220 (1991) 199–203.
[41] I. Reviakine, W. Bergsma-Schutter, A.N. Morozov, A. Brisson, Two-dimensional crystallization of annexin A5 on phospholipid bilayers and monolayers: a solid–solid phase transition between crystal forms, Langmuir 17 (2001) 1680–1686.
[42] A. Brisson, F. Bergesma-Schutter, F. Oling, O. Lambert, I. Reviakine, Two-dimensional crystallization of proteins on lipid monolayers at the air–water interface and transfer to an electron microscopy grid, J. Cryst. Growth 196 (1999) 456–470.
[43] F. Oling, J. Sopkova-De Oliveira Santos, N. Govorukhina, C. Mazarès-Dubut, W. Bergsma-Schutter, G. Oostergetel, W. Keegstra, O. Lambert, A. Lewit-Bently, A. Brisson, Structure of membrane-bound annexin A5 trimers: a hybrid cryo-EM–X-ray crystallography study, J. Mol. Biol. 304 (2000) 561–573.
[44] M.A. Swairjo, M.F. Roberts, M.B. Compos, J.R. Dedman, B.A. Seaton, Annexin V binding to the outer leaflet of small unilamellar vesicles leads to altered inner-leaflet properties: ^{31}P- and ^{1}H-NMR studies, Biochemistry 33 (1994) 10944–10950.
[45] H.L. Casal, H.H. Mantsch, F. Paltauf, H. Hauser, Infrared and ^{31}P-NMR studies of the effect of Li^{+} and Ca^{2+} on phosphatidylserines, Biochim. Biophys. Acta Lipids Lipid Metab. 919 (1987) 275–286.
[46] H.L. Casal, H.H. Mantsch, H. Hauser, Infrared studies of fully hydrated saturated phosphatidylserine bilayers: effect of Li^{+} and Ca^{2+}, Biochemistry 26 (1987) 4408–4416.
[47] M.A. Swairjo, N.O. Coucha, M.A. Kaetzel, J.R. Dedman, B.A. Seaton, Ca^{2+}- bridging mechanism and phospholipid head group recognition in the membrane-binding protein annexin-V, Nat. Struct. Biol. 2 (1995) 968–974.